BIOCHEMISTRY
including biophysical chemistry & molecular biology

Article

pubs.acs.org/biochemistry

Multistep, Eight-Electron Oxidation Catalyzed by the Cofactorless Oxidase, PqqC: Identification of Chemical Intermediates and Their Dependence on Molecular Oxygen

Florence Bonnot,[†,§] Anthony T. Iavarone,[†,§] and Judith P. Klinman*[,†,‡,§]

[†]Department of Chemistry, [‡]Department of Molecular and Cell Biology, and [§]California Institute for Quantitative Biosciences (QB3), University of California, Berkeley, California 94720, United States

ABSTRACT: The final step of the biosynthesis of prokaryotic cofactor PQQ is catalyzed by PqqC, a cofactorless oxidase that brings about a ring closure and overall eight-electron oxidation of its substrate. Time-dependent acid quenching and subsequent high-performance liquid chromatography separation and mass spectrometric analyses of reaction mixtures were performed to correlate the structures of intermediates with previously observed UV−visible signatures. The reaction is composed of four stepwise oxidations: three steps use O_2 as the two-electron acceptor, and the fourth uses hydrogen peroxide (H_2O_2). The chemical nature of the intermediates, the stoichiometry of the reaction, and their dependence on the oxygen concentration indicate that the third oxidation uses the product, H_2O_2, from the preceding step to produce water. The last oxidation step can also be studied separately and is a reaction between O_2 and $PQQH_2$ trapped in the active site. This oxidation is approximately 10 times slower than the reoxidation of $PQQH_2$ in solution. From the order of the four oxidation steps and their sensitivity to O_2 concentration, we propose a progressive closure of the active site as the enzyme proceeds through its catalytic cycle.

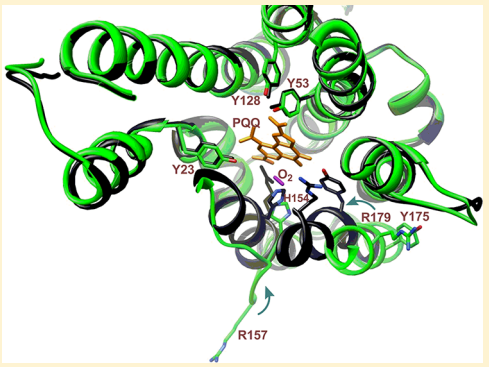

Pyrroloquinoline quinone [4,5-dihydro-4,5-dioxo-1*H*-pyrrolo[2,3-*f*]quinoline-2,7,9-tricarboxylic acid (PQQ)] is an aromatic, tricyclic *o*-quinone that serves as a cofactor for a large number of prokaryotic dehydrogenases found predominantly in Gram-negative bacteria.[1−3] PQQ belongs to the quinone family of enzymatic cofactors and has remarkable antioxidant properties.[4−6] Like all identified quinone cofactors, PQQ is derived from a ribosomally encoded precursor.[5] However, unlike the other described quinone cofactors, topaquinone (TPQ),[7] tryptophan tryptophylquinone (TTQ),[8] lysyl tyrosylquinone (LTQ),[9] and cysteine tryptophylquinone (CTQ),[10] which are generated *in situ* within their cognate proteins, PQQ is peptide-derived and is freely dissociable from its site of catalytic function.[5]

The biosynthesis of PQQ is a complex process and is catalyzed by gene products pqqA−F in *Klebsiella pneumoniae*.[11] All of the carbon and nitrogen atoms in PQQ derive from a conserved tyrosine and glutamate located near the C-terminus of peptide substrate PqqA.[12] The final step of PQQ formation is catalyzed by PqqC (Figure 1) and involves a ring closure and eight-electron oxidation of AHQQ [3a-(2-amino-2-carboxyethyl)-4,5-dioxo-4,5,6,7,8,9-hexahydroquinoline-7,9-dicarboxylic acid] (structure 1, Scheme 1).[13,14] As shown in Scheme 1, AHQQ must undergo a two-electron oxidative ring closure (A) followed by three additional two-electron oxidation steps (BI−BIII). X-ray studies of a mutant form of PqqC support ring closure as the initial step in AHQQ oxidation,[15,16] while the order of reactions BI−BIII is currently unknown. The stoichiometry of the reaction has been well-characterized, and the reaction occurs via the production of only 2 molar equiv of hydrogen peroxide (H_2O_2),

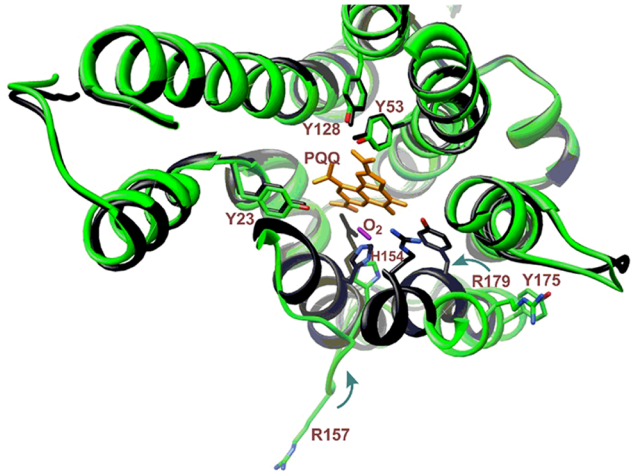

Figure 1. Image of WT PqqC without PQQ (green) (Protein Data Bank entry 10TV) in the open conformation and WT PqqC with PQQ (black) (Protein Data Bank entry 10TW) in the closed conformation. PQQ is colored orange, and the O_2 or H_2O_2 present in the active site is colored purple. A subset of the active site residues surrounding the PQQ are labeled in dark red. Note how the conformational change brings R157, R179 and Y175 into the active site.

Received: March 13, 2013
Revised: May 28, 2013

   dx.doi.org/10.1021/bi4003315 | *Biochemistry* XXXX, XXX, XXX−XXX

Scheme 1. Reaction of WT PqqC with AHQQ[a]

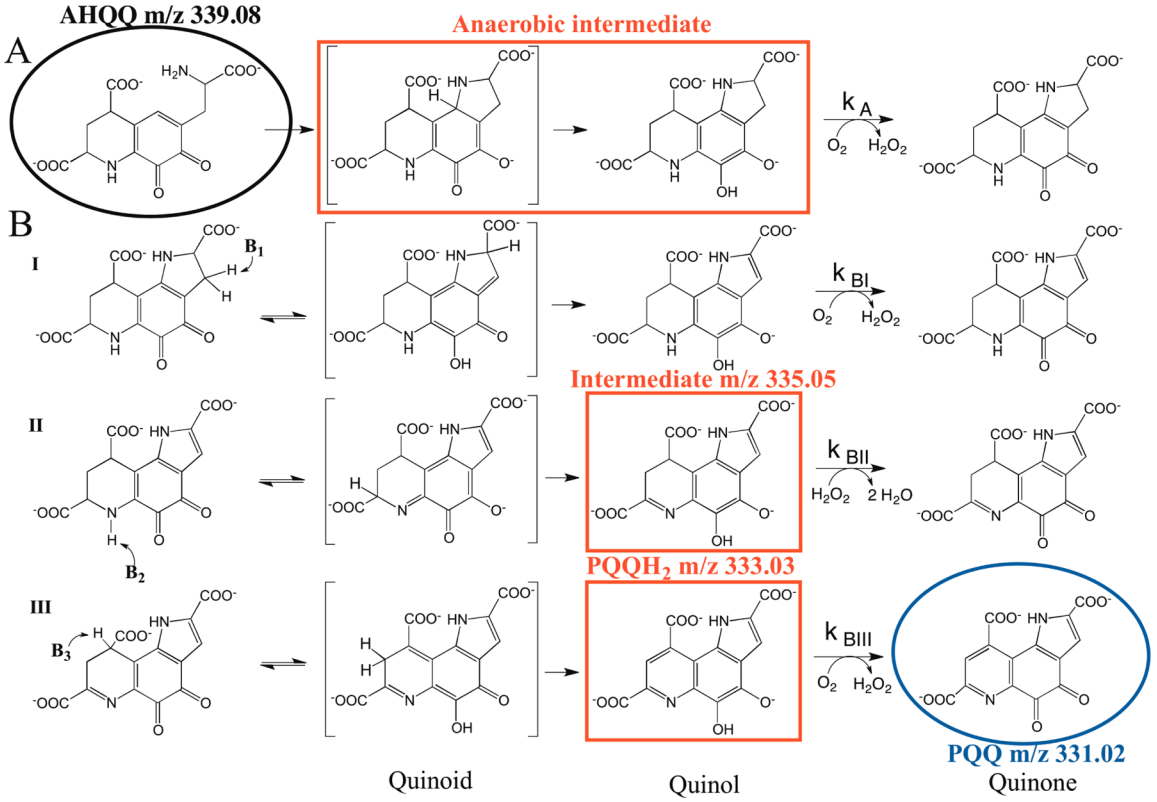

[a]The species observed in acid quench experiments at 5% O_2 are boxed in red. While these are illustrated as anions, mass spectrometric analyses were of the acidified species. Note that species detected anaerobically are also seen at the lowest O_2 level (5%) studied.

implicating bound hydrogen peroxide as the electron acceptor in either step BI or BII;[13] the biochemical detection of the final products, H_2O_2 and PQQ during a single turnover of PqqC further indicates that O_2 is the electron acceptor in the final product-forming step (BIII).[13] The absence of any requirement for an external cofactor or metal raises very intriguing questions regarding how O_2 is activated in this metal and cofactor free active site.

In this work, we sought to identify the substrate-derived intermediates formed during a single turnover of PqqC catalysis and to understand the impact of different oxygen concentrations on their distribution. The results allow us to determine the intermediates that accumulate during the reaction as a function of O_2 concentration and to establish the order of the different oxidations. X-ray crystallographic studies of PqqC show two conformations for PqqC; the free enzyme is open, with the active site solvent-exposed, whereas the addition of PQQ leads to significant reorganization and a more closed active site, Figure 1.[13] The dependence of the various reaction steps on oxygen concentration, the order of the different oxidations, and the intermediates that accumulate during the reaction all suggest that the enzyme undergoes a progressive closure at its active site in the course of the conversion of AHQQ to PQQ.

METHODS

Chemical and Molecular Biological Reagents. Buffers, salts, general reagents, and culture media were obtained from Sigma-Aldrich and Fisher Scientific and were of the highest available purity. Nickel-nitrilotriacetic acid (Ni-NTA) resin was purchased from Qiagen. PQQ was purchased from Fluka. AHQQ was purified from *pqqC* mutant strain EMS12 of *Methylobacterium extorquens* AM1 as described previously.[14] The concentration of AHQQ was determined spectrophotometrically at pH 7 by averaging the concentrations determined at three wavelengths with the following extinction coefficients: 15.7 mM^{-1} cm^{-1} at 222 nm, 8.26 mM^{-1} cm^{-1} at 274 nm, and 2.01 mM^{-1} cm^{-1} at 532 nm.

Expression and Purification of PqqC. Plasmids were constructed in pET29 with kanamycin resistance and a C-terminal His tag. PqqC was expressed and purified as described previously.[13] A single band was seen on a sodium dodecyl sulfate−polyacrylamide gel electrophoresis gel, and Ni-NTA column chromatography provided >95% pure enzyme. The expression for PqqC without a His tag was identical, but after the dialysis, the PqqC His tag was cut using a thrombin kit from Novagen (catalog no. 69022-3). The protein was incubated with the thrombin overnight at 4 °C, and the tag was removed with the Ni-NTA column and the thrombin via filtration after being mixed with streptavidin agarose. PqqC, without the His tag, exhibits the same level of activity with AHQQ as PqqC with the His tag.

Single-Turnover Kinetics Monitored by UV−Vis Spectroscopy. The enzyme (50 μM) was mixed with substrate, AHQQ (20 μM), in 100 mM potassium phosphate buffer (pH 8.0) in a total volume of 100 μL. The mixture was transferred to a microcuvette, and UV−vis spectra were recorded within 10 s of mixing. The temperature of the reaction mixture was maintained at 20 °C. Spectra were acquired at predetermined time points and the data exported to SPECFIT/32 for analysis. A baseline was obtained under identical conditions with enzyme but without AHQQ. Despite the baseline subtraction, the absorbance below 300 nm was very noisy and has been omitted

dx.doi.org/10.1021/bi4003315 | *Biochemistry* XXXX, XXX, XXX−XXX

in the data presentation. Anaerobic reactions were performed under the same conditions as described above. The enzyme and substrate were made anaerobic by three vacuum/nitrogen cycles on the freeze solution and brought into an anaerobic chamber (Plas Laboratories 855-AC glovebox). Protein samples were transferred into a microcuvette covered with a rubber septum, and the substrate was loaded into a gastight syringe before being removed from the anaerobic chamber. The substrate was injected through the septum and the solution thoroughly mixed immediately prior to the spectra being recorded.

Acid Quench Experiment. The enzyme (100 μM) was mixed with substrate, AHQQ (40 μM), in 100 mM potassium phosphate buffer (pH 8.0) in a total volume of 80 μL. The reaction was quenched by the addition of 4 μL of concentrated HCl. The reaction mixture was centrifuged for 5 min at 12000 rpm, and the supernatant was then loaded onto a C18 column equilibrated with 5% acetonitrile with 0.1% TFA. Reaction intermediates were eluted using a gradient of 5 to 20% acetonitrile over a 20 min period. The absorbance was monitored between 250 and 700 nm using a diode array detector. Fractions were collected and analyzed by mass spectrometry as described below.

Mass Spectrometry. Mass spectrometry analysis was performed using an LTQ Orbitrap XL mass spectrometer equipped with an electrospray ionization (ESI) source (Thermo Fisher Scientific, Waltham, MA) that was connected in-line with an Agilent (Santa Clara, CA) 1200 series autosampler and pump. Sample solutions contained in polypropylene autosampler vials sealed with septa caps (Wheaton, Millville, NJ) were loaded into the autosampler compartment prior to analysis. The injected sample (15 μL) was pumped to the ESI probe of the mass spectrometer using a flow of acetonitrile (50 μL/min). The connection between the autosampler and the ESI probe of the mass spectrometer was made using PEEK tubing [0.005 in. inner diameter × 1/16 in. outer diameter (Agilent)]. Mass spectra were recorded in positive ion mode using the Orbitrap mass analyzer, in profile format, with a resolution setting of 100000 (at m/z 400). Mass spectra were processed using Xcalibur version 2.0.7 SP1 (Thermo).

Determination of the K_d for $PQQH_2$. Binding of $PQQH_2$ to PqqC was measured fluorometrically. Assays were performed in 100 mM potassium phosphate buffer (pH 8.0) at room temperature. A fixed concentration of $PQQH_2$ was employed (100 nM), and the concentration of enzyme was varied. Samples were incubated for 5 min, and fluorescence emission was recorded at 333 nm (slit width of 5 nm) using an excitation wavelength at 282 nm (slit width of 5 nm). Data were fit to a quadratic binding isotherm (eq 1)

$$\Delta F = \Delta F_M([E]_T + [L]_T + K_d - \{[([E]_T + [L]_T + K_d)^2 - 4[E]_T[L]_T]^{0.5}\}/(2[E]_T)) \quad (1)$$

where ΔF equals the change in fluorescence between a given sample and the free ligand, ΔF_M equals the change in fluorescence at saturation, $[E]_T$ equals the total concentration of the enzyme in each sample, $[L]_T$ equals the total ligand concentration, and K_d is the dissociation constant of the enzyme–ligand complex. Data were fit using Kaleidagraph (Synergy Software).

The determination of the K_d (PQQ-PqqC) for the wild-type (WT) enzyme at different concentrations of O_2 was performed fluorometrically as previously described [15] in a closed cuvette.

Quinol Oxidation Assays. PQQ (100 μM) was anaerobically reduced using 1.25 equiv of dithiothreitol (125 μM). This reduced quinol was then bound to 125 μM PqqC enzyme anaerobically in 100 mM KP_i (pH 8.0) in a glovebox (Plas Laboratories 855-AC glovebox). A microcuvette fitted with a rubber stopper containing 80 μL of 100 mM KP_i (pH 8.0) was flushed for 20 min under a nitrogen/oxygen flow (the ratio of oxygen was determined using an oxygen electrode). The protein was transferred into a microcuvette fitted with a rubber stopper, and the substrate was loaded into a syringe and the needle inserted through the stopper into the top of the cuvette. The cuvette with the syringe attached was brought to the spectrophotometer, and the substrate was mixed thoroughly with the enzyme before spectra were recorded. The spectral traces were analyzed with SPECFIT. The data were fit to a single exponential to find the rate of oxidation of quinol to quinone.

RESULTS

Single-Turnover Kinetics of Wild-Type PqqC at Variable O_2 Concentrations, Monitored by UV–Vis Monitoring. Reactions were performed with excess enzyme (2.5 equiv) to ensure that all of the reactions that were monitored occurred from the E–S complex. Spectra at various time points during the WT PqqC reaction are shown in Figure 2. At all dioxygen concentrations between 0 and 1.14 mM, qualitative assessment shows a decay of substrate at 532 nm, concomitant with the appearance of a chromophore with a λ_{max} of ~318 nm. This species subsequently decays, and a direct precursor–product relationship with a new chromophore with a λ_{max} at 344 nm can be seen by the isosbestic point at 332 nm. The final chromophore represents enzyme-bound PQQ (Figure 2). Singular-value decomposition analysis yielded each individual spectral component, and the data were fit to an irreversible, two-consecutive-exponential model, which yielded observed rate constants that are dependent on O_2 concentration (Figure 3A,B). Compilation of the results was achieved via the global fitting procedure with SPECFIT (as described previously[15]). The concentration of dioxygen in the reaction mixtures clearly affects the kinetics. The formation of the reduced intermediate at 318 nm yields rate constants ranging from 0.2 to 1.5 min^{-1} at oxygen concentrations of 0–1.14 mM (Figure 3A), while the formation of the 344 nm species (PQQ) is slower and shows rate constants of 0–0.2 min^{-1} in 0–1.14 mM O_2 (Figure 3B). The apparent K_d values for O_2 during these two processes are also distinct:

$$\text{AHQQ} \xrightarrow[K_{d_{app}}(O_2)=0.51\pm0.16\text{mM}]{k_{1app}} 318\text{ nm} \xrightarrow[K_{d_{app}}(O_2)=0.05\pm0.02\text{mM}]{k_{2app}} 344\text{ nm}$$

Although the 318 nm intermediate represents a quinol,[15] there are four such species possible in the course of the overall reaction (Scheme 1). Identification of this intermediate was accomplished using acid quench techniques as described below.

Identification of the Reduced Quinol Intermediates at Varying O_2 Concentrations by Acid Quench. The reaction intermediates formed under the different experimental conditions were determined by a combination of high-performance liquid chromatography (HPLC) separation and mass spectrometry. The UV–vis spectra, retention times, and masses for the starting material and oxidized and reduced products, AHQQ, PQQ, and $PQQH_2$, respectively, at pH 2 were obtained by comparison with those of pure samples. Under the conditions established, AHQQ elutes at 11.5 min, occurs at m/z 339.08, and shows λ_{max} values of 275 and 510 nm; PQQ elutes at 16.9 min, occurs at m/z 331.02, and shows λ_{max} values of

dx.doi.org/10.1021/bi4003315 | Biochemistry XXXX, XXX, XXX–XXX

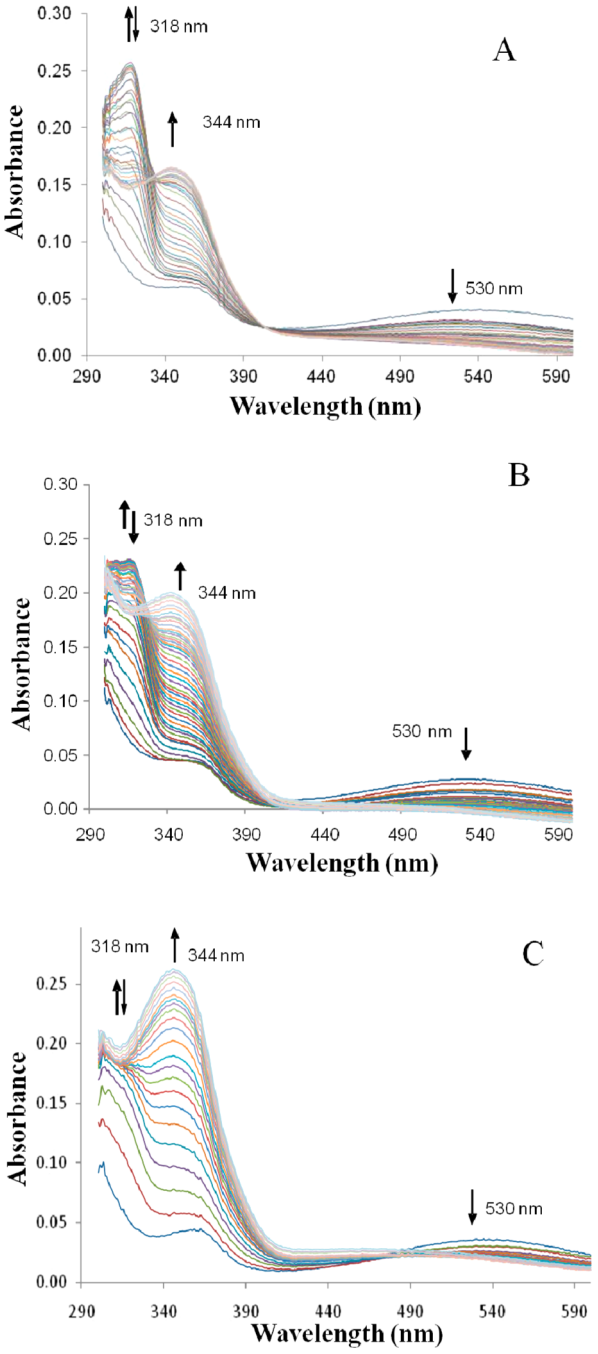

Figure 2. Reaction of WT PqqC with AHQQ (at concentrations of 50 and 20 μM, respectively) as a function of time in 0.1 M phosphate (pH 8) at 20 °C followed by UV−vis monitoring over 20 min. (A) At 4% O_2, k_1 = 0.27 min^{-1} and k_2 = 0.08 min^{-1}. (B) At 21% O_2, k_1 = 0.75 min^{-1} and k_2 = 0.13 min^{-1}. (C) At 100% O_2, k_1 = 1.4 min^{-1} and k_2 = 0.2 min^{-1}.

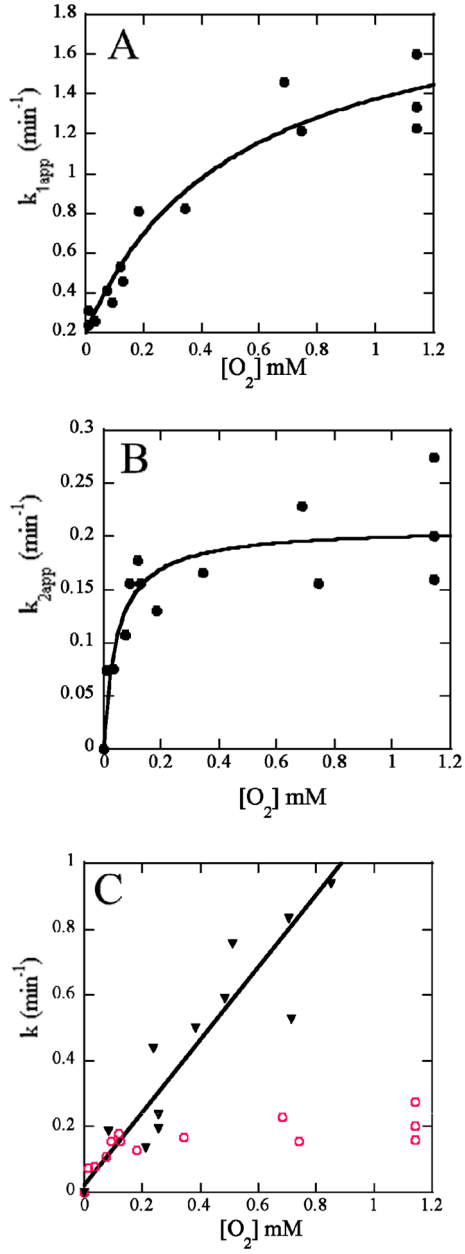

Figure 3. WT PqqC with AHQQ (at concentrations of 50 and 20 μM, respectively) as a function of O_2 concentration in 0.1 M phosphate (pH 8) at 20 °C followed by UV−vis monitoring and fit with SPECFIT. (A) $k_{1_{app}}$ describes the formation of the 318 nm species. (B) $k_{2_{app}}$ describes the formation of the 344 nm species. (C) Comparison of $k_{2_{app}}$ observed during the reaction of WT PqqC and AHQQ (red) and the kinetics of $PQQH_2$ reoxidation (black). For the latter, $PQQH_2$ is formed by reduction of PQQ by DTT and mixed with WT PqqC (30 μM PqqC and 20 μM $PQQH_2$) in different concentrations of O_2 in 0.1 M phosphate (pH 8) at 20 °C followed by UV−vis monitoring at 344 nm.

247 and 349 nm with a shoulder at 270 nm; and $PQQH_2$ elutes at 20.1 min, occurs at m/z 333.03, and shows a λ_{max} value of 320 nm (Figure 4A).

At 21% O_2 (240 μM O_2), the rapid decay of substrate is concomitant with the appearance of a chromophore with a λ_{max} at 303 nm (m/z 335.05) at an elution time of 17.5 min. This initial intermediate subsequently decays, and a second intermediate with the same mass, elution time, and spectrum as PQQ forms (Figure 4B). Additionally, once PQQ begins to accumulate, a small amount of $PQQH_2$ with a λ_{max} of 320 nm (m/z 333.03), eluting at 20.1 min, is observed (this can be seen in the 3 min reaction shown in Figure 4B). The intermediate occurring at m/z 335.05 may represent the quinol or the quinone. To identify which intermediate was accumulating during the reaction of AHQQ with PqqC, the intermediate was mixed with phenylhydrazine, a derivatization agent known to react readily with quinones.[17] The reaction of phenylhydrazine with PQQ and $PQQH_2$ has previously been studied. The reaction with PQQ leads to the formation of a chromophore

dx.doi.org/10.1021/bi4003315 | *Biochemistry* XXXX, XXX, XXX−XXX

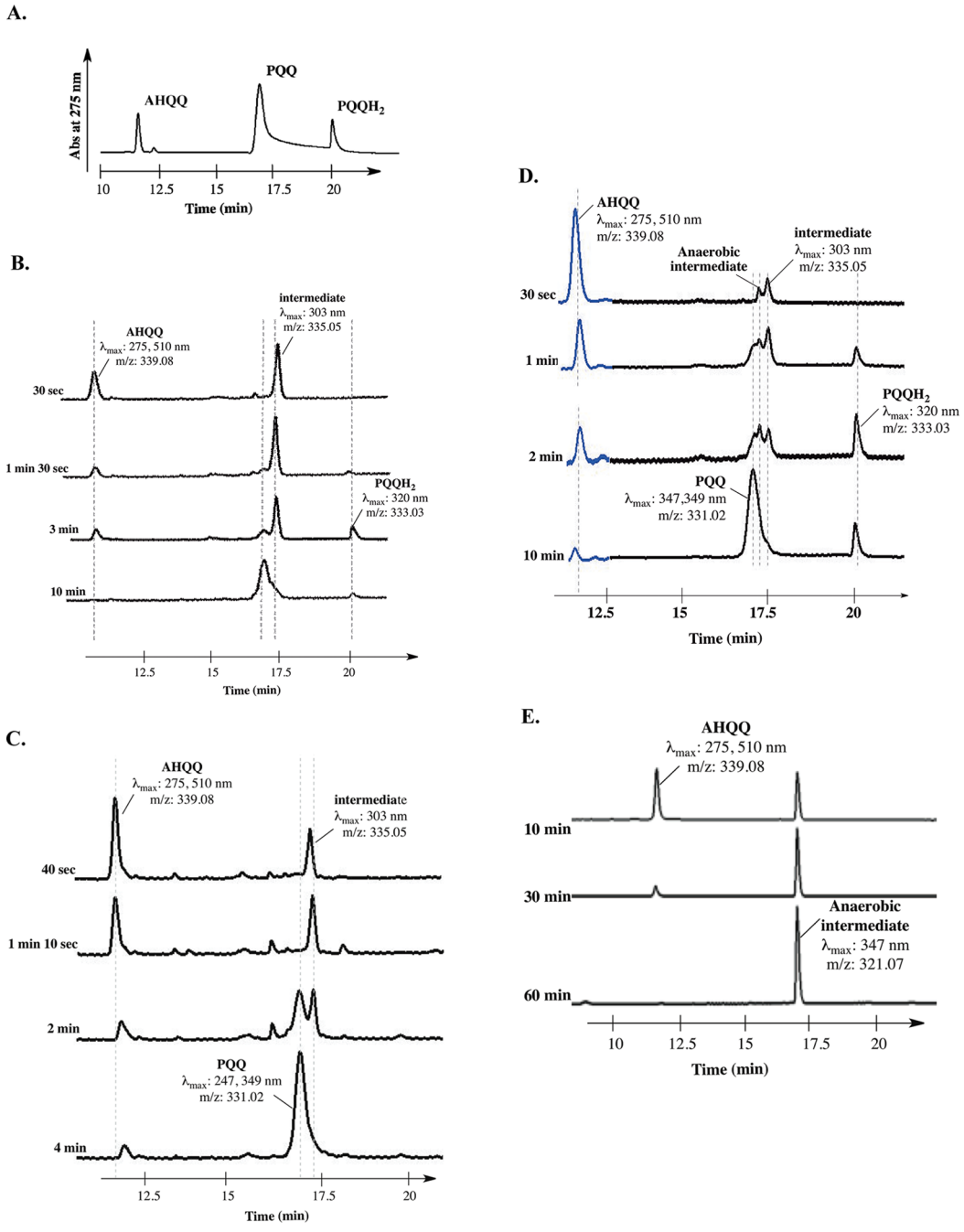

Figure 4. HPLC traces for the reactant, intermediates, and product under a variety of conditions. (A) HPLC traces monitored at 275 nm of a standard mixture (AHQQ, PQQ, and $PQQH_2$). The elution times were as follows: 11.4 min for AHQQ, 16.9 min for PQQ, and 20.1 min for $PQQH_2$. (B) HPLC traces monitored at 275 nm for WT PqqC reaction with AHQQ (100 and 40 μM, respectively) in 0.1 M phosphate (pH 8) at 20 °C in 20% O_2 quenched with HCl at different times (30 s, 90 s, 3 min, and 10 min), centrifuged, and loaded onto HPLC. The elution times were as follows: 11.4 min for AHQQ, 16.9 min for PQQ, 17.5 min for the intermediate, and 20.1 min for $PQQH_2$. (C) HPLC traces monitored at 275 nm for WT PqqC reaction with AHQQ (100 and 40 μM, respectively) in 0.1 M phosphate (pH 8) at 20 °C in 100% O_2 quenched with HCl at different times (40 s, 70 s, 2 min, and 4 min), centrifuged, and loaded onto HPLC. The elution times were as follows: 11.4 min for AHQQ, 16.9 min for PQQ, 17.5 min for intermediate, and 20.1 min for $PQQH_2$. (D) HPLC traces monitored at 275 nm before 12.5 min (blue) and at 340 nm after 12.5 min (black) of WT PqqC reaction with AHQQ (100 and 40 μM, respectively) in 0.1 M phosphate (pH 8) at 20 °C in 5% O_2 quenched with HCl at different times (30 s, 1 min, 2 min, and 10 min), centrifuged, and loaded onto HPLC. The elution times were as follows: 11.4 min for AHQQ, 16.9 min for PQQ, 17.2 for an anaerobic intermediate, 17.5 min for an intermediate, and 20.1 min for $PQQH_2$. (E) HPLC traces monitored at 275 nm for WT PqqC reaction with AHQQ (100 and 40 μM, respectively) in 0.1 M phosphate (pH 8) at 20 °C in the absence of O_2 quenched with HCl at different times (10, 30, and 60 min), centrifuged, and loaded onto HPLC. The elution times were as follows: 11.4 min for AHQQ and 17.2 min for an anaerobic intermediate.

with a λ_{max} of 315 nm, with the absorbance intensity being proportional to the concentration of PQQ, whereas incubation of phenylhydrazine with $PQQH_2$ leads to no apparent reaction.[17] When this same reaction was performed with the intermediate at m/z 335.05, no spectral changes were observed. This indicates that the intermediate with a λ_{max} at

dx.doi.org/10.1021/bi4003315 | *Biochemistry* XXXX, XXX, XXX−XXX

303 nm and m/z 335.05 is a quinol and not a quinone species (the quinol of BII in Scheme 1).

At 100% O_2 (1.14 mM O_2), the data are similar to what is observed for the reaction in 21% O_2, though the reaction proceeds more rapidly and without any detectable $PQQH_2$ (Figure 4C). At high O_2 concentrations, the only intermediate that accumulates during the reaction is the quinol BII shown in Scheme 1.

At 5% O_2 (57 μM O_2), the accumulation of $PQQH_2$ is much more pronounced than at 21% O_2 (Figure 4D). Almost all the substrate is $PQQH_2$ at 3 min of reaction. Indeed, the rate of $PQQH_2$ reoxidation appears to be the most affected by the change in O_2 concentration. The cumulative data, thus, strongly point toward an oxidation of bound $PQQH_2$ by O_2 and not H_2O_2. In the beginning of the reaction at 5% O_2, a very small amount of an intermediate with a λ_{max} at 347 nm (m/z 321.07) can also be seen eluting at 17.2 min. This intermediate is observed in the anaerobic reaction between PqqC and AHQQ (Figure 4E), with a rate of formation of ~0.2 min^{-1} (see below) and can be assigned to quinol A. The low level of quinol A is consistent with comparable rates for its formation and decay. The reaction intermediates detected by acid quench at 57 μM O_2 are boxed in red in Scheme 1. In contrast to these data, only a single intermediate was detected during the UV–vis single-turnover kinetics, most likely because the spectra of bound quinols A, BII, and $PQQH_2$ are too similar to be distinguished from one another.

Comparison of UV–Vis and Acid Quench under Anaerobic Conditions. Under anaerobic conditions, the initial steps of the PQQ reaction were probed using the established UV–vis and acid quench techniques. The anaerobic reaction intermediates have been previously characterized by UV–vis spectroscopy and display the following absorption maxima.[13]

$$\text{E-AHQQ} \rightarrow \underset{\text{E}-(\text{quinoid})}{344\text{ nm}} \rightarrow \underset{\text{E}-(\text{quinol})}{318\text{ nm}}$$

In the WT enzyme, the rate of transformation of E–quinoid to E–quinol is very fast (i.e., not observable). The reaction spectra in this study indicate formation of the species with a λ_{max} of 318 nm at a rate of 0.2 min^{-1}. Quenching of the anaerobic reaction by acid and subsequent HPLC separation and mass spectral analysis of the reaction products shows a single intermediate with an elution time of 17.2 min, a λ_{max} of 347 nm, and an ion at m/z 321.07 (Figure 4E). This species appears concomitant with the decay of the substrate (AHQQ), and occurs at the same rate as the appearance of the λ_{max} = 318 nm species seen via UV–vis spectroscopy.

Neither the mass (m/z) nor λ_{max} of the acid quench-derived anaerobic intermediate matched the values expected from the UV–vis spectra for the protonated form of quinol A in Scheme 1. The mass (m/z) is 18 Da smaller than expected, and the UV–vis spectrum exhibits a red-shifted absorbance. We propose that the acidic conditions of the quench catalyze a second reaction, in which the initial cyclization step of AHQQ is followed by an intramolecular reaction between the carboxylate at C9 and nitrogen of the five-membered quinoid/quinol ring to form a stable lactam product:

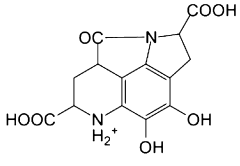

This structure is consistent with both the observed mass and red-shifted UV–vis spectrum of the anaerobic intermediate.

Reoxidation of Exogenous $PQQH_2$ as a Function of O_2 Concentration. The last step of the reaction catalyzed by PqqC is one in which the reduced product, $PQQH_2$, is converted to PQQ. It is possible to probe and compare the disappearance of exogenously added $PQQH_2$ at different O_2 concentrations. Estimation of the K_d for added $PQQH_2$ was first conducted by following the protein fluorescence as a function of added $PQQH_2$ (excitation at 282 nm, emission at 333 nm, under anaerobic conditions). WT PqqC was found to bind $PQQH_2$ less tightly than PQQ (K_d = 50 nM for $PQQH_2$, and K_d = 2.0 nM for PQQ[15]). However, under the conditions used in the $PQQH_2$ oxidation assay (20 μM $PQQH_2$ with 25 μM enzyme), all the $PQQH_2$ is predicted to be bound to the enzyme. Concentrated $PQQH_2$ was first incubated with enzyme anaerobically to ensure that $PQQH_2$ is fully bound prior to the addition of O_2 and then diluted with a buffer with a known oxygen concentration in a closed cuvette. Quinols are known to reoxidize to quinones in buffer in air;[20] in the presence of PqqC, the rate of $PQQH_2$ reoxidation is found to be ~8 times slower than in buffer. Although the enzymatic reaction was conducted over a range of O_2 concentrations, a saturating concentration of O_2 was never achieved (Figure 3C). Below 200 μM O_2, the rate of oxidation of $PQQH_2$ is very close to the measured $k_{2_{app}}$, consistent with a similar rate-determining process for the oxidation of either AHQQ or added $PQQH_2$ in this O_2 concentration range (Figure 2). In contrast, above 200 μM O_2, where the rate of the oxidation of bound $PQQH_2$ becomes more rapid, the enzymatic oxidation of the substrate AHQQ is limited by another step. These results are fully compatible with the changes in reaction intermediates observed using acid quench methodology at different O_2 concentrations.

We have previously reported that the PqqC–$PQQH_2$ complex could be oxidized under anaerobic conditions with exogenously added H_2O_2, as well as molecular oxygen.[18,19] More recent studies show that this consumption of H_2O_2 occurs in the absence of $PQQH_2$ and leads to a time-dependent evolution of O_2 as measured on an O_2 electrode. Because the earlier and current studies use His-tagged PqqC, we prepared PqqC without its His tag and re-examined reoxidation of $PQQH_2$ by H_2O_2 using UV–vis monitoring, finding a rate (0.04 ± 0.005 min^{-1}) that is <10% of what was previously reported.[19] Apparently, the His tag itself is capable of a reaction with H_2O_2 to liberate O_2, possibly because of the binding of a trace redox-active metal to the tag itself. Much of the earlier observation of oxidation of $PQQH_2$ by exogenous H_2O_2 was, thus, likely due to the O_2 liberated via a side reaction. In the study presented here, conducted in the absence of added H_2O_2, the initial level of H_2O_2 during the reaction of AHQQ with PqqC is very low. At later times, as the product peroxide accumulates, this may undergo some oxidation via reaction at the His tag. However, the oxidation of bound $PQQH_2$ by product peroxide can be neglected. Re-evaluation of the ratio for consumption of O_2 to production of H_2O_2 using PqqC without His tag leads to a result identical to the previously reported result.[13]

As an alternative way of examining the possibility of the saturation of the enzyme by O_2 in the presence of bound product, the K_d for the interaction of PQQ with PqqC was determined as a function of increasing O_2 concentration. Consistent with the kinetic measurements for $PQQH_2$ oxidation, the K_d for PQQ increases in a linear fashion with O_2 concentration, reaching a value that is approximately 10 times larger at >1 mM O_2 relative to that under the anaerobic condition (Figure 5). O_2 appears to

dx.doi.org/10.1021/bi4003315 | Biochemistry XXXX, XXX, XXX–XXX

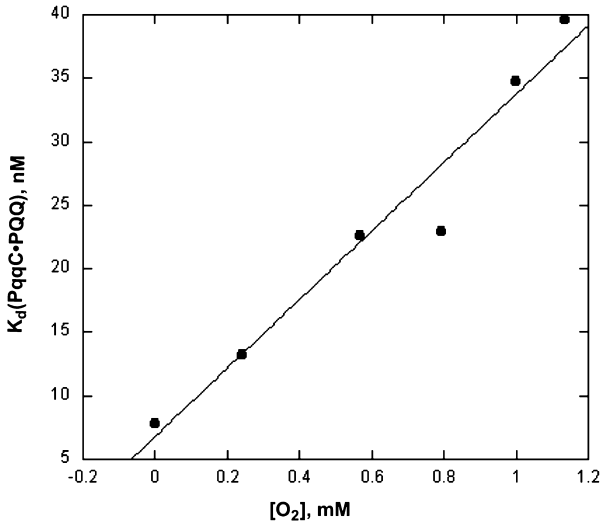

Figure 5. K_d values of the WT PqqC−PQQ complex determined by fluorescence in 0.1 M phosphate (pH 8) at different dioxygen concentrations. Both the λ_{max} and intensity for the emission are different for bound and free PQQ.[14]

be unable to saturate the enzyme in the concentration range studied (from 0 to 1.2 mM), though the sensitivity of the binding of PQQ to O_2 levels is consistent with a binding site for the gas at the active site, as implicated from the X-ray structure determined in the presence of both PQQ and O_2 (Figure 1).

DISCUSSION

As shown in Scheme 1, AHQQ must undergo a two-electron oxidative ring closure (A), followed by three additional two-electron oxidation steps (BI−BIII) using two molecules of O_2 and one molecule of H_2O_2.[13] While the first of the four steps in this single-turnover process has been identified as a ring closure (A)[17] and the last involves the oxidation of the reduced product (BIII), the chemical steps in BI and BII may occur either as shown or in the reverse order. The net reaction was previously monitored solely by UV−vis spectroscopy at a single oxygen concentration (air). The expectation of similar absorbance properties for the quinoid and quinol intermediates in steps A through BI−BIII made identification of the species that accumulated during the reaction impossible. In this study, we have turned to acid quench−mass spectrometry experiments that, when combined with UV−vis measurements across a range of O_2 concentrations, provide considerable insight into the nature of the accumulated intermediates and, by inference, the nature of the rate-determining steps.

By UV−vis spectroscopy, the rates of reaction of PqqC with a range of O_2 levels can be accommodated by two kinetic traces, $k_{1_{app}}$ (representing the appearance of the quinol species at 318 nm) and $k_{2_{app}}$ (representing the disappearance of quinol at 318 nm and the appearance of quinone at 344 nm) (Figure 2). These kinetic traces ($k_{1_{app}}$ and $k_{2_{app}}$) at each O_2 concentration are, in fact, the sum of different rates according to the acid quench experiments. Comparison of m/z values for the isolated species in air versus 5 and 100% O_2 shows that the quinol of BII (Scheme 1) is the only intermediate that accumulates at all measured O_2 concentrations. In air, the reduced product, $PQQH_2$, is also seen, whereas 5% O_2 leads to both the reduced product and a small amount of quinol A (i.e., the substrate subsequent to ring closure but lacking any oxidative modification). The latter is identical to the first quinol (A), formed under anaerobic conditions.

The fact that the accumulation of the intermediates varies when the reaction is conducted at different O_2 concentrations indicates that, in fact, the UV−vis traces at the three experimental oxygen concentrations represent different processes. At low O_2 concentrations (≤5%), $k_{1_{app}}$ represents the sum of the formation of quinol A, quinol BII, and $PQQH_2$. At 21% O_2, quinol A no longer accumulates, a small amount of $PQQH_2$ is observed, and the majority of the product is quinol BII. The maximal level of $PQQH_2$ observed during the catalysis is <8% of the level of PQQ formed at the end of the reaction (calculated using the extinction coefficients of $PQQH_2$ at 320 nm and PQQ at 275 nm and the HPLC traces at these wavelengths at 3 and 10 min for the determination of the amount of $PQQH_2$ and PQQ, respectively). At this O_2 concentration, while the formation of $PQQH_2$ is still detectable, its contribution to $k_{1_{app}}$ is quite small. At high O_2 concentrations, $k_{1_{app}}$ is a direct observation of the formation of quinol BII, which is the only intermediate observed at 100% O_2. One very interesting observation from these comparative analyses is the rate of appearance of quinol ($k_{1_{app}}$) at high O_2 concentrations is more rapid than the rate of anaerobic formation of quinol A, which appears with a rate constant of 0.2 s^{-1}. This means that the anaerobic portion of the reaction must be affected by the presence of O_2, accelerating the formation of quinol A, whose formation would otherwise be rate-limiting at the elevated O_2 concentrations. This result implicates an interaction (binding) between O_2 and PqqC that alters a portion of the reaction that is chemically independent of O_2, namely, the conversion of AHQQ to quinol A. The presence of an O_2 binding pocket near the bound substrate or product has previously been inferred from the X-ray crystal structure of PqqC in the presence of PQQ[17] (Figure 1) and is further implicated from the data in Figure 5.

The earlier determination of the stoichiometry of oxygen consumption in the net PqqC reaction had indicated that one of the four steps in Scheme 1 must involve the consumption of the product H_2O_2, formed in a previous step. The resulting prediction of an O_2-independent step is, in fact, confirmed and identified in this study. The only species seen to accumulate at all O_2 concentrations is quinol BII. According to the acid quench experiments, the second kinetic trace observed by UV−vis spectroscopy ($k_{2_{app}}$) represents the disappearance of quinol BII at high O_2 concentrations, together with a small contribution from the disappearance of quinol A (5% O_2) and $PQQH_2$ (5 and 21% O_2). Once the accumulated levels of quinol A and $PQQH_2$ approach zero, the disappearance of BII has become independent of O_2. This could have meant that the disappearance of BII with O_2 had a very low K_m but was intrinsically slow. However, as we argue below, quinol BII is assigned to the species that reacts with hydrogen peroxide rather than O_2.

Ideally, these studies would have allowed a direct monitoring of the disappearance of each quinol in Scheme 1 as a function of O_2 concentration, to distinguish its reaction with O_2 from that with H_2O_2. In the case of the first oxidation (of quinol A), there is no H_2O_2 present and this reaction must proceed with O_2. Further, the fact that the amount of quinol A observed at 5% O_2 is already very low makes its contribution to $k_{2_{app}}$ negligible at all O_2 levels. Quinol BI was never observed in these studies, making it impossible to correlate its disappearance with a varying O_2 concentration. We were, however,

dx.doi.org/10.1021/bi4003315 | *Biochemistry* XXXX, XXX, XXX−XXX

able to follow the disappearance of $PQQH_2$ as a function of O_2 concentration. We accomplished this by reducing PQQ with DTT, mixing the resulting $PQQH_2$ (20 μM) with PqqC (30 μM), and monitoring its reoxidation at 344 nm (Figure 3C, black line). It can be seen that the O_2 dependence of the direct oxidation of the bound $PQQH_2$ is very different from the O_2 dependence seen in $k_{2_{app}}$ and fails to show saturation under any condition (Figure 3C). This property will be related to the protein structure in the ensuing discussion. From a kinetic perspective, the data show a much faster rate for $PQQH_2$ oxidation above 21% O_2 than for the oxidation of quinol BII, consistent with the absence of $PQQH_2$ by acid quench at elevated O_2 concentrations:

$$\text{E-quinol BII} \xrightarrow[k_{BII}]{\text{Limited step for } k_{2_{app}} \text{ at } >0.2 \text{ mM } O_2} \text{E-PQQH}_2 \xrightarrow{k_{BIII}} \text{E} - \text{PQQ}$$

Using the measured values for k_{BIII} as a function of O_2 concentration, it was possible to estimate the rate for the disappearance of BII at all O_2 concentrations according to eq 2:

$$k_{2_{app}} = k_{BII}k_{BIII}[O_2]/k_{BII} + k_{BIII}[O_2] \quad (2)$$

The analysis indicates that all of the change in $k_{2_{app}}$ as a function of O_2 concentration arises from the oxidation of bound $PQQH_2$, and that k_{BII} is fully independent of O_2 concentration.

The unique dependence of each step of the PqqC reaction sequence on O_2 or H_2O_2 suggests a deliberate property for each of the oxidation steps. In particular, the following questions are raised: (i) Why does the enzyme import three molecules of dioxygen and not two or four? (ii) Why does the reoxidation of BII occur using H_2O_2? (iii) Why is the oxidation of enzyme-bound $PQQH_2$ so slow at the ambient O_2 concentration? Crystallographic studies of PqqC have shown two conformations for PqqC: an open form with the active site exposed to solvent and a closed form that occurs when PQQ is bound (Figure 1). The closure of the active site of PqqC must occur either during the binding of AHQQ, along the reaction path, or via a combination of both processes. The dependence of the reaction sequence on O_2 suggests that this closure takes place during each of the chemical steps. For the two initial oxidation steps, O_2 can easily access the active site and rapidly oxidize the bound quinols; only the formation of quinol A emerges as a potentially slow step at >50 μM O_2. After these two oxidation steps, the active site appears to have become quite closed. This provides a rationale for the use of bound peroxide during the third oxidation step. It appears that PqqC encounters a "log jam" at its BII intermediate, preventing either egress of the product H_2O_2 from the previous step or the binding of O_2. This enforces a reductive step that uses hydrogen peroxide rather than O_2 in an intrinsically slower process. The oxidation of bound $PQQH_2$ offers even more of a challenge, with regard to access to O_2. The nonsaturating nature of O_2 during this step indicates a process that is first-order in O_2 up to 1.14 mM. In this case, the product (H_2O) from the previous reaction may be impeding access and/or binding of the O_2 required for the final step. Importantly, however, a previous study of the net PqqC stoichiometry showed that only one molecule of H_2O_2 was released to the buffer directly. The detection of the second mole of peroxide product required acid denaturation of PqqC. For reasons not yet understood, the oxygen-derived product from the last reaction binds tightly, despite the fact that the O_2 reaction is fully second-order. This suggests that only upon formation and oxidation of $PQQH_2$ does the enzyme enter into its fully closed form, trapping bound peroxide in the proximity of PQQ. This is consistent with the approximately 10-fold tighter binding of PQQ than $PQQH_2$ to PqqC. Taken together, the aggregate data strongly support a progressive closure of the active site during catalysis: at each step, the active site becomes more insulated from solvent.

In all the cofactor-independent oxidases studied, the substrate plays the key role in the activation of O_2,[20,21] with the abstraction of a proton from the organic substrate by a catalytic base initiating the oxidative process. In some cases, the presence of a specific O_2 pocket has been shown, ideally located above the substrate.[22] While none of these enzymes has, thus far, indicated any direct activation of O_2, we note that the active site of PqqC contains positively charged and H-bonding residues near the ascribed O_2 pocket; these side chains may play an important electrostatic role in stabilizing the superoxide anion during those steps that use O_2 as the immediate oxidant.

We now address a possible physiological relevance of the observed slow oxidation of PqqC-bound $PQQH_2$. As noted, the oxidation of $PQQH_2$ is, in fact, slower on the enzyme than in buffer (cf. ref 18). With regard to *in vivo* function, enzyme-bound $PQQH_2$ may, thus, be the anticipated product. A low concentration of O_2 in the bacterial species that make PQQ would lead to an accumulation of enzyme-bound $PQQH_2$ rather than PQQ. In the context of the very low (nanomolar) K_d value for binding of PQQ to PqqC, the accumulation of the 25-fold weaker binding-reduced product may be an evolved function to ensure production of sufficient levels of the free cofactor. This feature may be a particularly important accompaniment to the postulated progressive closure of the enzyme as it proceeds through its catalytic cycle. For the future, it should be particularly informative to obtain and contrast an X-ray structure for PqqC in complex with its reduced rather than oxidized product.

■ CONCLUSION

This study has demonstrated the isolation and identification of reaction intermediates during the final step of PQQ biogenesis, catalyzed by PqqC. The comparison of acid quench-derived species with UV−vis traces as a function of O_2 concentration shows that oxidant utilization is distinct in each of the four catalytic steps. One of the four steps has been shown to use H_2O_2 rather than molecular dioxygen, while a second step undergoes a first-order reaction with O_2. These properties are attributed to a stepwise closure of the enzyme from an open to fully closed form that is not complete until the final chemical step of the reaction. The very slow rate of formation of enzyme-bound PQQ from its precursor $PQQH_2$ at the ambient O_2 concentration suggests that $PQQH_2$ is the physiologically relevant product of this biosynthetic pathway.

■ AUTHOR INFORMATION

Corresponding Author

*E-mail: klinman@berkeley.edu. Telephone: (510) 642-2668.

Funding

Financial support was provided by National Institutes of Health Grants GM025765 to J.P.K. and 1S10RR022393-01 to A.T.I.

Notes

The authors declare no competing financial interest.

■ ABBREVIATIONS

AHQQ, 3a-(2-amino-2-carboxyethyl)-4,5-dioxo-4,5,6,7,8,9-hexahydroquinoline-7,9-dicarboxylic acid; PQQ, pyrroloquinoline quinone; $PQQH_2$, dihydroquinone PQQ; WT, wild type.

REFERENCES

(1) Anthony, C. (2001) Pyrroloquinoline quinone (PQQ) and quinoprotein enzymes. *Antioxid. Redox Signaling 3*, 757−774.

(2) Arakawa, K., Sugino, F., Kodama, K., Ishii, T., and Kinashi, H. (2005) Cyclization mechanism for the synthesis of macrocyclic antibiotic lankacidin in *Streptomyces rochei*. *Chem. Biol. 12*, 249−256.

(3) Goodwin, P. M., and Anthony, C. (1998) The biochemistry, physiology and genetics of PQQ and PQQ-containing enzymes. *Adv. Microb. Physiol. 40*, 1−80.

(4) Rucker, R., Chowanadisal, W., and Nakano, M. (2009) Potential physiological importance of pyrroloquinoline quinone. *Alternative Medicine Review: A Journal of Clinical Therapeutic 14*, 268−277.

(5) Arnison, P. G., Bibb, P. G., Bierbaum, M. G., et al. (2013) Ribosomally synthesized and post-translationally modified peptide nature products: Overview and recommendations for a universal nomenclature. *Nat. Prod. Rep. 30*, 106−160.

(6) He, K., Nukada, H., Urakami, T., and Murphy, M. P. (2003) Antioxidant and pro-oxidant properties of pyrroloquinoline quinone (PQQ): Implications for its function in biological systems. *Biochem. Pharmacol. 65*, 67−74.

(7) Janes, S. M., Mu, D., and Wemmer, D. (1990) A new redox cofactor in eukaryotic enzymes-6-hydroxydopa at the active site of bovine serum amine oxidase. *Science 248*, 981−987.

(8) McIntire, W. S., Wemmer, D. E., Christoserdov, A., et al. (1991) A new cofactor in a prokaryotic enzyme tryptophan tryptophylquinone as the redox prosthetic group in methylamine dehydrogenase. *Science 252*, 817−824.

(9) Wang, S., Mure, M., Medzihradszky, K. F., and Burlingame, A. L. (1996) A crosslinked cofactor in lysyl oxidase: Redox function for amino acid side chains. *Science 273*, 1078−1084.

(10) Datta, S., Mori, Y., Takagi, K., Kawaguchi, K., Chen, Z. W., et al. (2001) Structure of a quinoprotein in amine dehydrogenase with an uncommon redox cofactor and highly unusual crosslinking. *Proc. Natl. Acad. Sci. U.S.A. 98*, 14268−14273.

(11) Shen, Y. Q., Bonnot, F., Imsand, E. M., RoseFigura, J. M., Sjölander, K., and Klinman, J. P. (2012) Distribution and properties of the genes encoding the biosynthesis of the bacterial cofactor, pyrroloquinoline quinone. *Biochemistry 51*, 2265−2275.

(12) Houck, D. R., Hanners, J. L., and Unkefer, C. J. (1991) Biosynthesis of pyrroloquinoline quinone. 2. Biosynthetic assembly from glutamate and tyrosine. *J. Am. Chem. Soc. 113*, 3162−3166.

(13) Magnusson, O. T., Toyama, H., Saeki, M., Rojas, A., Reed, J. C., Liddington, R. C., Klinman, J. P., and Schwarzenbacher, R. (2004) Quinone biogenesis: Structure and mechanism of PqqC, the final catalyst in the production of pyrroloquinoline quinone. *Proc. Natl. Acad. Sci. U.S.A. 101*, 7913−7918.

(14) Magnusson, O. T., Toyama, H., Saeki, M., Schwarzenbacher, R., and Klinman, J. P. (2004) The structure of a biosynthetic intermediate of pyrroloquinoline quinone (PQQ) and elucidation of the final step of PQQ biosynthesis. *J. Am. Chem. Soc. 126*, 5342−5343.

(15) Magnusson, O. T., RoseFigura, J. M., Toyama, H., Schwarzenbacher, R., and Klinman, J. P. (2007) Pyrroloquinoline quinone biogenesis: Characterization of PqqC and its H84N and H84A active site variants. *Biochemistry 46*, 7174−7186.

(16) Puehringer, S., RoseFigura, J. M., Metlitzky, M., Toyama, H., Klinman, J. P., and Schwarzenbacher, R. (2010) Structural studies of mutant forms of the PQQ-forming enzyme PqqC in the presence of product and substrate. *Proteins 78*, 2554−2562.

(17) Mure, M., Nii, K., Inoue, T., Itoh, S., and Ohshino, Y. (1990) The reduction of coenzyme PQQ with hydrazines. *J. Chem. Soc., Perkin Trans. 2*, 315−320.

(18) Itoh, S., Ohshiro, Y., and Agawa, T. (1986) Reaction of reduced PQQ ($PQQH_2$) and molecular oxygen. *Bull. Chem. Soc. Jpn. 59*, 1911−1914.

(19) RoseFigura, J. M., Puehringer, S., Schwarzenbacher, R., Toyama, H., and Klinman, J. P. (2011) Characterization of a protein-generated O_2 binding pocket in PqqC, a cofactorless oxidase catalyzing the final step in PQQ production. *Biochemistry 50*, 1556−1566.

(20) Fetzner, S., and Steiner, R. A. (2010) Cofactor-independent oxidases and oxygenases. *Appl. Microbiol. Biotechnol. 86*, 791−804.

(21) Gabison, L., Chopard, C., Colloc'h, N., Peyrot, F., Castro, B., El Hajji, M., Altarsha, M., Monard, G., Chiadmi, M., and Prangé, T. (2011) X-ray, ESR, and quantum mechanics studies unravel a spin well in the cofactorless urate oxidase. *Proteins 79*, 1964−1976.

(22) Colloc'h, N., Gabison, L., Monard, G., Altarsha, M., Chiadmi, M., Marassio, G., Sopkova-de Oliveira Santos, J., El Hajji, M., Castro, B., Abraini, J. H., and Prangé, T. (2008) Oxygen pressurized X-ray crystallography: Probing the dioxygen binding site in cofactorless urate oxidase and implications for its catalytic mechanism. *Biophys. J. 95*, 2415−2422.

dx.doi.org/10.1021/bi4003315 | *Biochemistry* XXXX, XXX, XXX−XXX